Competitive Adsorption of H_2O and CO_2 in 2-Dimensional Nano-Confinement: GCMD Simulations of Cs- and Ca-Hectorite

Narasimhan Loganathan, Geoffrey M. Bowers, A. Ozgur Yazaydin, Andrey G. Kalinichev, R. James Kirkpatrick

THE JOURNAL OF PHYSICAL CHEMISTRY C

C: Surfaces, Interfaces, Porous Materials, and Catalysis

Competitive Adsorption of HO and CO in 2-Dimensional Nano-Confinement: GCMD Simulations of Cs- and Ca-Hectorite

Narasimhan Loganathan, Geoffrey M Bowers, A. Ozgur Yazaydin, Andrey G. Kalinichev, and R. James Kirkpatrick

J. Phys. Chem. C, **Just Accepted Manuscript** • DOI: 10.1021/acs.jpcc.8b06602 • Publication Date (Web): 21 Sep 2018

Competitive Adsorption of H_2O and CO_2 in 2-Dimensional Nano-confinement: GCMD Simulations of Cs- and Ca-Hectorite

Narasimhan Loganathan[1,*] *Geoffrey M. Bowers*[2], *A. Ozgur Yazaydin*[1,3], *Andrey G. Kalinichev*[4] *and R. James Kirkpatrick*[1,5]

[1] Department of Chemistry, Michigan State University, East Lansing, Michigan 48824, United States

[2] Department of Chemistry and Biochemistry, St. Mary's College of Maryland, St. Mary's City, Maryland 20686, United States

[3] Department of Chemical Engineering, University College London, London, WC1E7JE, United Kingdom

[4] Laboratoire SUBATECH (UMR 6457 - Institut Mines-Télécom Atlantique, Université de Nantes, CNRS/IN2P3), 44307, Nantes, France

[5] Department of Earth and Environmental Sciences, Michigan State University, East Lansing, Michigan 48824, United States

[*] **Corresponding author e-mail:** naresh20@msu.edu

Telephone: (+1)517-353-1106

Abstract

The intercalation of H_2O, CO_2, and other fluid species in expandable clay minerals (smectites) may play a significant role in controlling the behavior of these species in geological carbon sequestration and enhanced petroleum production and has been the subject of intensive study in recent years. This paper reports the results of a computational study of the effects of the properties of the charge balancing, exchangeable cations on H_2O and CO_2 intercalation in the smectite mineral, hectorite, in equilibrium with an H_2O-saturated supercritical CO_2 fluid under reservoir conditions using Grand Canonical Molecular Dynamics (GCMD) methods. The results show that the intercalation behavior is greatly different for the cations with relatively low hydration energies and high affinities for CO_2 (here Cs^+) than for cations with higher hydration energies (here Ca^{2+}). With Cs^+, CO_2 intercalation occurs in a 1-layer structure and does not require H_2O intercalation, whereas with Ca^{2+} the presence of a sub-monolayer of H_2O is required for CO_2 intercalation. The computational results provide detailed structural, dynamical and energetic insight into the differences in intercalation behavior and are in excellent agreement with *in situ* experimental XRD, IR, quartz crystal microbalance, and NMR results for smectite materials obtained under reservoir conditions.

Introduction

Clay minerals are important components of the deep sedimentary formations that are potential reservoirs for geological CO_2 sequestration and shale/tight gas production.[1-16] The competitive interaction of CO_2 and H_2O with clays is, thus, central to understanding fluid behavior in these situations. The common smectite and mixed-layer illite-smectite clay minerals contain expandable interlayer galleries that contain intercalated charge balancing cations and variable numbers of fluid molecules. The partitioning of CO_2 and H_2O between the intergranular pore fluid and the interlayer galleries may be significant in controlling the overall transport and physical properties of the host rock and has been a topic of substantial recent experimental and computational study.[16-42] Due to the presence of two basal surfaces separated by less than one to a few nm, the structure and dynamics of fluids nano-confined in the interlayer galleries are substantially different than on external clay surfaces (interparticle pores) or in the bulk fluid phase. Recent experimental and computational modeling studies have clearly shown that the clay swelling behavior depends strongly on the nature of the charge balancing cation (characterized by the CO_2 and H_2O solvation energies) and on the composition and location of the permanent structural charge of the clay.[43-57]

Experimental and computational modeling studies have shown that at reservoir conditions the amount of intercalated CO_2 and its structural, dynamical, and energetic properties depend on the basal spacing and the solvation energies of the charge-balancing cation with H_2O and CO_2 in smectite interlayers under supercritical conditions ($scCO_2$, T_c~31ºC, P_c~73 bar).[17-42] X-ray diffraction (XRD) studies at pressurized CO_2 conditions by Giesting et al.[18,19] showed that increase (expansion) of the basal spacing of the common smectite, montmorillonite, depends on the initial interlayer H_2O content. Similar studies by Schaef et al.[26,28] at 323 K and 90 bar fluid pressure have confirmed that the intercalation of CO_2 in Na-, Ca- and Mg-montmorillonite is possible only when there is at least a sub-

monolayer amount of H_2O that props open the interlayer. For these cations, solvation by H_2O is energetically more favorable than by CO_2. The *in situ* infrared (IR) results of Loring et al.[29-31] for Na-montmorillonite confirmed that a similar minimum content of co-adsorbed H_2O is necessary to facilitate CO_2 intercalation and demonstrated that at 323 K and 90 bar maximum CO_2 intercalation occurs when the amount of co-adsorbed H_2O corresponds to a monolayer (1L) hydrate structure. More recently, the *in situ* XRD, IR and nuclear magnetic resonance (NMR) results of Bowers et al.[17] at 323K and 90 bar showed that the solvation properties of the exchangeable cation (Na^+, Cs^+ or Ca^{2+}) significantly affect the structure, dynamics, and energetics of intercalated CO_2 in the similar smectite mineral, hectorite. The results show that interlayers containing large, monovalent cations that have similar solvation energies for H_2O and CO_2 (such as Cs^+)[58] intercalate CO_2 even under experimentally dry conditions after vacuum drying. In contrast, with Na^+ and Ca^{2+} CO_2 intercalation requires at least a sub-1L of H_2O to prop open the interlayers. For all these hectorites, the interlayer CO_2 content increases up to the 1L structure and decreases at higher H_2O contents, as for montmorillonite at the same conditions.[18,26,29] These results emphasize the importance of having molecular scale understanding of the structure, dynamics, and energetics of H_2O and CO_2 in the interlayers of smectites with exchangeable cations spanning a range of solvation energies with H_2O and CO_2.

Computational molecular modeling studies for Na-smectites are in good agreement with the experimental results showing that CO_2 intercalation requires the presence of at least a sub-1WL H_2O layer.[33-37,40] Grand Canonical Monte Carlo (GCMC) simulations by Botan et al.[33] also suggest a stable bilayer (2L) hydrate structure (basal spacing ~15.0Å) for Na-montmorillonite at 348 K and 125 bar in contact with H_2O-saturated $scCO_2$. The GCMC simulations of Rao et al.[37] reported a higher interlayer CO_2 mole fraction for Na-montmorillonite with lower structural charge than with higher ones (-0.75 $|e|$ vs. -1.0 $|e|$) at a given relative humidity (R.H.) at 323 K and 90 bar. Gibbs Ensemble Monte Carlo studies of

Makaremi et al.[36] showed how the location of the structural charge sites in the smectite framework T-O-T layer structure alters the equilibrium basal spacing and energetics of Na-smectites at 348 K and 125 bar. Our previous grand canonical molecular dynamics (GCMD) simulations showed that temperature (323-368 K) and pressure (90-150 bar) have little impact on the structure and dynamics of interlayer CO_2 in Na-hectorite in contact with H_2O saturated $scCO_2$.[40]

There are, however, few computational modeling studies that examine the effect of cation solvation energy on the partitioning of H_2O and CO_2 between smectite interlayers and bulk fluid and its interlayer structure, dynamics, and energetics in the supercritical regime. To our knowledge, the only such study is that of Kadoura et al.,[34] who explored the influence of Na^+, Ca^{2+} and Mg^{2+} on CO_2 intercalation in montmorillonite at 323 K and 90 bar using GCMC. The results show that the interlayer CO_2 mole fraction is very similar with all these cations at R.H.s $\geq$ 60%, consistent with their high affinity for H_2O. In contrast, our recent *in situ* XRD, IR and NMR experiments and GCMD simulations with montmorillonite and hectorite have shown that cations with low hydration energies (e.g., Cs^+, K^+, NH_4^+) permit CO_2 intercalation even in the absence of H_2O at 323 K and 90 bar in smectites, whereas those cations with higher hydration energies (e.g., Na^+, Ca^{2+}, Mg^{2+}) do not.[41,42] Energetically, the results show that the clay-cation interactions play a dominant role in determining the overall intercalation behavior, suggesting that further studies should be performed for cations with a greater range of size, CO_2 and H_2O solvation energies.[41,42]

We address this gap here by examining the intercalation behavior of H_2O and CO_2 in hectorite containing a cation with a low hydration energy (Cs^+) and one with a high hydration energy (Ca^{2+}) at 323 K and 90 bar in equilibrium with H_2O-saturated $scCO_2$ using GCMD simulations.[40-42] Cs^+ and Ca^{2+} are representative of cations with greatly different hydration energies and charge/radius ratios,[48,53,58] and they have greatly different CO_2/H_2O intercalation

behavior.[17] The results here are in excellent agreement with experimental data of Bowers et al.[17] and provide a basis for their detailed molecular scale structural, dynamic, and energetic interpretation and understanding.

The primary reason for using hectorite rather than montmorillonite is that samples of natural hectorite with a very low Fe content are available, and such samples were used in NMR experiments to reduce paramagnetic effects on the probe nuclei.[17] Both hectorite and montmorillonite develop their layer charge dominantly in the octahedral layer, and previous experimental NMR, IR, XRD, neutron scattering and simulation studies have shown that their intercalation behavior is very similar when fully hydroxylated and possessing identical layer charge.[17-23, 25-54]

Simulation Details

Hectorite is a 2:1 trioctahedral smectite that develops its negative structural layer charge by isomorphic substitution of Li^+ for Mg^{2+} in the octahedral layer. The simulated hectorite model has a structural formula of $M^+(Mg_5Li)Si_8O_{20}(OH)_4$. There are no tetrahedral substitutions in this model, in accordance with the experimental sample that contains a negligible fraction (0.25%) of isomorphic Al^{3+}/Si^{4+} substitution.[59] However, there are two important differences between the natural sample used in our experiments and the simulated model: (i) the model has 30% higher layer charge, and (ii) the simulated octahedral layer has only OH^- groups, whereas the natural sample has ~ 55% F^- for OH^- substitution.[17,46,47] The hydration behavior of synthetic fluoro-hectorite has been discussed previously.[60]

The simulation supercells for the Cs- and Ca-hectorite models consist of 16 crystallographic unit cells of hectorite (4 × 2 × 2) and include two interlayer galleries with surface areas of ~20.9 Å × 18.2 Å (*a*=*b*=*c*: 90º) that are large enough to overcome any finite size effects. The isomorphic Li^+ for Mg^{2+} substitutions were introduced only after constructing the supercell. This procedure provides a quasi-disordered pattern with different arrangements

of Li^+ ions in the octahedral layer. Li-O-Li linkages are forbidden in this procedure in accordance with the generalization of Lowenstein's rule.[61] The initial structure has the charge compensating cations placed randomly in the interlayer region. Further details about this hectorite model are described elsewhere.[40,42,49,51]

We performed the GCMD[62] simulations in the grand canonical ensemble at 323 K and 90 bar using methods described previously.[40,42] Briefly, the interlayer basal spacings were varied from 9.2 Å to 18.0 Å at an interval of 0.2 Å. The interlayer galleries were constrained to maintain the same interlayer spacing along the *z*-dimension in each simulation run. However, the simulations allow the lateral movement of the T-O-T layers along the *x* and *y* directions without disrupting the structure or changing the basal spacing. This is because the minimum energy interlayer structure depends strongly on the relative positions of adjacent T-O-T layers and varies with the nature of the interlayer cation and the number of intercalated fluid molecules.[33,40] All the simulations were performed using the GCMD module embedded in the simulation package, RASPA.[63] The interatomic interactions for the clay structure and the exchangeable cations are calculated using the *CLAYFF* force field,[64] which is widely used in clay interfacial simulations. The H_2O and CO_2 molecules were represented by the rigid versions of the SPC[65] and EPM2[66] models, respectively. Three-dimensional periodic boundary conditions were employed with a cutoff of 9.0 Å for short range non-electrostatic interactions, and the long-range electrostatic interactions were computed using Ewald summation[67] with an accuracy of 10^{-6}.

The composition of the virtual reservoir representing the bulk H_2O-CO_2 fluids corresponds to the H_2O-saturated CO_2-rich phase at the simulated pressure (90 bar) and temperature (323 K). The values were obtained from the experimental solubility data of Spycher et al.[68] (x_{H2O} = 0.0041 x_{CO2} = 0.9959). Fugacities required to calculate the probability of acceptance and deletion moves of the fluid species (f_{H2O} = 0.231: f_{CO2} = 0.654) were obtained

using the Peng-Robinson equation of state.[69] Further details of the GCMD approach and data analysis have been discussed in our previous papers. [40,42,49,51,70,71]

Results and Discussion

Adsorption Profiles and Energetics

The computed intercalation behavior of CO_2 and H_2O are very different in the Cs- and Ca-hectorites (Figures 1a -1c). For both systems, neither H_2O nor CO_2 intercalate at basal spacings less than 10.2 Å, but their behaviors are very different as the interlayers expand (Figures 1a and 1b). For Ca-hectorite, H_2O adsorption begins at 10.2 Å and reaches a plateau at ~11.0 Å, where CO_2 intercalation begins (Figure 1a). With increasing basal spacing, the amount of intercalated CO_2 increases, reaches a maximum at 12.8Å, gradually decreases at larger spacings, and finally reaches an approximately constant value of 0.2 CO_2/unit cell at spacings > ~16.0 Å. In contrast, the amount of intercalated H_2O remains almost constant at spacings between 11.0 Å and 12.8 Å, and then increases almost linearly with further increase of the interlayer spacing. Based on our previous studies of hydrated Ca-hectorite without CO_2,[51] the amount of H_2O (~3 molecules/unit cell) in the plateau region corresponds to approximately 1/3 of that needed for a full monolayer hydrate structure. This result is in good agreement with experimental studies that show CO_2 intercalation in Ca-hectorite begins only with H_2O present in the interlayer.[17] The decrease in interlayer CO_2 mole fraction with increasing H_2O content is consistent with previous IR spectroscopic data for hectorite and similar smectites (montmorillonite).[17,29-31] The experimentally determined Ca-hectorite basal spacings of ~12.6 Å and ~15.9 Å correspond to 1L and 2L structures, respectively, and are in very good agreement with the simulated values of 12.8 Å and 16.2 Å.[17] These 1L and 2L distances are also comparable to those from our recent MD simulations of hydrated Ca-hectorite without CO_2 at ambient conditions.[51] Importantly, the adsorption profiles of CO_2 and H_2O reported here are similar to our previous studies on Na-hectorite under identical thermodynamic conditions.

This similarity emphasizes the critical role played by the H_2O molecules in propping open the interlayer region to allow CO_2 intercalation when the interlayer cations have relatively high hydration energies.[40,58]

In contrast, for Cs-hectorite neither H_2O nor CO_2 intercalate at basal spacings <11.1 Å. With increasing basal spacing beyond this value, CO_2 intercalation increases up to 12.5 Å, decreases at larger values, has a shallow local minimum near 14.2 Å, and reaches a nearly constant value of ~0.3 CO_2/unit cell at spacings > 16.0 Å (Figure 1b). Significant H_2O intercalation begins only at ~13.0 Å, near the maximum of CO_2 intercalation, and increases with increasing basal spacing. The amount of intercalated H_2O at spacings < 13.0 Å is negligible (1.5%), consistent with the experimentally observed intercalation of CO_2 in Cs-hectorite under fully dry conditions with a basal spacing of 12.2 Å, indicative of an anhydrous 1L structure.[17] At basal spacings > 13.2 Å, the decrease in CO_2 intercalation is compensated by increasing H_2O. The adsorption profiles and the interlayer distance at which CO_2 intercalation begins reported here are very similar those in our earlier study of Cs-hectorite exposed to dry $scCO_2$[42] up to 13.2 Å, suggesting that the intercalation behavior of CO_2 is not significantly affected by the presence of H_2O in the bulk fluid phase reservoir. Similar increases in interlayer H_2O content at larger spacings have been reported previously in simulations of hydrated Cs-hectorite and other smectites,[49,54] although such expanded structures are not observed experimentally.

The calculated immersion energies for Cs-hectorite (Figure 1c) show a global minimum at a basal spacing of ~12.5 Å, indicating that the 1L structure is the thermodynamically stable state for this phase in equilibrium with H_2O-saturated $scCO_2$ at 323 K and 90 bar, in agreement with the experimental results.[17] In contrast, for Ca-hectorite the energy minimum near the 1L structure is poorly localized. The immersion energies decrease beyond the 1L structure and reach a minimum at 16.2 Å, corresponding to a 2L structure. Further increase in basal spacing

shows little variation in energy, consistent with experimental observations that higher hydration states for Ca-hectorite are possible, depending upon the thermodynamic activity of H_2O.[17] Most importantly, these results clearly demonstrate that the thermodynamically stable state of Ca-hectorite in equilibrium with H_2O-saturated $scCO_2$ has a much larger basal spacing than Cs-hectorite under the same conditions, consistent with experimental XRD measurements.[17] The qualitative behavior of the immersion energies of Ca-hectorite are also consistent with our previous MD simulations of hydrated Ca-hectorite without CO_2.[51] Ideally, formation of the stable energy structures can be obtained by computing the disjoining pressure and swelling free energy calculations.[72,73] However, the results of Young et al.[71] for hydrated smectites indicate that conclusions drawn from the immersion energies and free energies are comparable to each other. The use of immersion energies to investigate the equilibrium states of smectites have been discussed elsewhere for H_2O adsorption and is extended to CO_2 in our studies.[49,51,70] Importantly, the thermodynamic stable states obtained using the immersion energy criterion in our earlier studies of Na-hectorite under identical simulated conditions are comparable with the conclusions based on swelling free energies reported using the similar smectite mineral, montmorillonite.[33,36,37,40,42] Therefore, we conclude that the energetic features of the immersion energy plots are good indicators of the thermodynamically stable states.

The computed interlayer CO_2 mole fractions in Cs- and Ca-hectorite are in good agreement with the ranges estimated from *in situ* high *T* and *P* experimental studies conducted at similar *T* and *P* conditions[17] (Table 1). For Cs-hectorite, our simulations indicate a CO_2 mole fraction of 0.98 at the equilibrium 1L basal spacing of 12.5 Å, in reasonable agreement with the upper-range experimental value of 0.82 estimated from the intensities of the spinning side bands (SSBs) in ^{13}C NMR spectra and the IR observed H_2O/cation ratio.[17] Similarly, for Ca-hectorite the computed CO_2 mole fractions of 0.34 for the 1L (12.8 Å) structure and 0.02 for the 2L (16.2 Å) structure are within the ranges estimated from NMR/IR data, though we note

that the 2L result is close to what was reported as the minimum interlayer mole fraction for this sample.[17] The differences between the experimental and computed results for both Cs- and Ca-hectorite are mostly likely associated with uncertainty in the IR-derived H_2O/cation ratio due difficulty in resolving signal from CO_2 sorbed on external surfaces and in interlayers, the layer charge differences between SHCa-1 and the model (-0.75 |*e*| vs -1.0 |*e*|), and the use of a fully hydroxylated hectorite model in contrast to the extensively fluorinated experimental sample.[17] Because of the higher structural charge used in the simulations, the model requires more Ca^{2+} ions to charge compensate the surface. Due to the high hydration energy of Ca^{2+},[58] more H_2O molecules are adsorbed in the interlayer region to hydrate these Ca^{2+} ions leading to less available space for CO_2 intercalation in the simulation. The effect of charge was been reported previously by Rao et al.[37] for a similar smectite mineral, montmorillonite. In addition, the XRD profiles of Dazas et al.[74] clearly indicate that adsorption of H_2O is less for fluorinated hectorite compared to hydroxylated hectorite. As a result, there is probably more interlayer space available for CO_2 intercalation in the experimental sample than in our simulated model.[17] Because the natural samples inevitably adsorb fluid species on external surfaces, the simulations provide specific insight into the interlayer fluid composition and dynamics.

Importantly, for the 1L structures, which for each cation have the greatest interlayer CO_2 contents, both Cs- and Ca-hectorite have more interlayer CO_2 than Na-hectorite, as also observed in the experimental high *T* and *P* IR results.[17,40] Recent GCMC simulation studies by Kadoura et al.[34] show similar behavior, with Ca- and Mg-montmorillonite having higher CO_2 mole fractions than Na- montmorillonite at a given R.H. The interlayer CO_2 mole fractions from our studies for Ca-hectorite are similar to the reported values by Kadoura et al.[34] for Ca-montmorillonite, despite our simulations having a higher layer charge.

Interlayer Structure

As for the adsorption isotherms, the atomic density profiles (ADPs) of the intercalated species as functions of distance normal to the basal surface are greatly different for Cs- and Ca-hectorite (Figures 2a-2c). For the 1L structures, the presence of H_2O in Ca-hectorite leads to a more complex interlayer structure than for Cs-hectorite, which has only ~1.5% interlayer H_2O and, thus, does not yield an observable H_2O ADP. For both 1L phases, the ADPs of the cation (Ca^{2+} or Cs^{+}), C_{CO2} and O_{CO2} are characterized by single peaks located at the mid-plane of the interlayer (Figures 2a and 2c) coordinating directly with the basal surface. This arrangement is the same as in Cs-hectorite exposed to dry $scCO_2$ at the same T and P.[42] For the 1L structure of Ca-hectorite, the nearest neighbor Ca^{2+} coordination shell (Figure 3d) consists of 6.0 H_2O (3 associated with each surface) and 2.0 O_b (one from each surface), and the ADPs of O_{H2O} and H_{H2O} are characterized by 4 and 5 peaks respectively. As shown in our previous simulations of hydrated Ca-hectorite without CO_2,[51] these distributions indicate two different adsorption environments for H_2O, one close to the basal surface and the other near the mid-plane of the interlayer. The H_2O molecules closer to the surface are coordinated to the oxygen atoms of the basal surface, O_b, through both of their H_{H2O}. Those near the mid-plane are coordinated to the O_b atoms through only one H_{H2O} at a time. The H_2O APDs have been discussed in more detail in our earlier study.[51] Although the 2L structure is the thermodynamically stable state for Ca-hectorite in contact with H_2O-saturated $scCO_2$ at our conditions, the structure and dynamics for the 1L state are relevant, because experimental XRD studies show that it occurs in the presence of H_2O-undersatruated $scCO_2$ (low R.H. conditions).[17] We use the basal spacing of 12.8 Å to represent the 1L structure because it has the maximum amount of interlayer CO_2 and a complete 1L structure. This 1L structure is comparable to the experimental structure of Ca-hectorite upon exposure to dry $scCO_2$ (0 % R.H.), in which the interlayer spacing corresponds to 1L regime and has a maximum CO_2 content.[17]

In the 2L structure of Ca-hectorite (Figure 2b), Ca^{2+} occurs at the mid-plane of the interlayer ~4.8 Å from the two basal surfaces and is coordinated by 8.0 H_2O (4 associated with each basal surface) in a square antiprism arrangement (Figure 3f), consistent with recent high *T-P* NMR studies.[17] In contrast, the C_{CO2} and O_{CO2} ADP peaks at 3.0 Å and 6.7 Å show that the CO_2 molecules are in direct coordination with the basal surfaces. In addition, the broad shoulders for O_{CO2} at ~2.2 Å and ~7.5 Å, even closer to the nearest basal surface, shows that the CO_2 molecules probe more orientations and are less dynamically restricted in the 2L structure than in the 1L structure. As in the 1L structure, the H_2O molecules at 2.8 Å from each basal surface are coordinated to the O_b atoms through one H-atom. In contrast, H_2O molecules in the mid-plane region (at ~5.0 Å) are coordinated only to other H_2O molecules and the Ca^{2+}, and not to the basal surfaces. The Ca^{2+} and CO_2 distributions are in reasonable agreement with previous simulations of Ca-montmorillonite in contact with $scCO_2$ under similar conditions.[34] However, our hectorite simulations show only one ADP peak for Ca^{2+} in the 1L and 2L structures, and consequently different H_2O profiles. This difference is probably due to the presence of tetrahedral charge resulting from Al for Si substitution in the montmorillonite model used by Kadoura et al.[34] and to the smaller layer charge (-0.8 |*e*|) compared to our model (-1.0 |*e*|). The presence of tetrahedral charge can greatly change the interlayer adsorption, structure, and dynamics of CO_2 and H_2O molecules, as discussed by Makaremi et al.[36] It should be noted that the interlayer arrangements of CO_2 molecules in Ca-hectorite in both the 1L and 2L structures are similar to the comparable systems with Na^+, although the H_2O distributions are different because the larger H_2O content in the present study leads to a more ordered interlayer H_2O structure than in Na-hectorite.[40]

In the 1L structure of Cs-hectorite and the 1L and 2L structures of Ca-hectorite, the computations show that intercalated CO_2 molecules are oriented with the average position of their O-C-O vectors parallel to the basal surface (Figure 2d) and that they undergo librational

motion around an axis perpendicular to their O-C-O axis. The values 0 and ±1 for $P(\cos\vartheta)_{CO2}$ correspond to parallel and perpendicular orientation of CO_2 with respect to the plane of the basal surface, respectively. These results are in full agreement with the interpretation of spinning sideband patterns in *in situ* experimental ^{13}C MAS NMR spectra.[17] In addition, the calculations show that the O-C-O axies probe a range of angles, demonstrating wobbling motion with respect to the basal surfaces. For Ca-hectorite, the angular distribution is larger for the 2L structure (between ~±0.8) than for the 1L structure (between ~±0.6). The range of orientations probed by the O-C-O vectors in the 1L structure of Cs-hectorite is essentially identical to that of the same hectorite model exposed to dry $scCO_2$ under similar conditions.[42] This is as expected due to the very low H_2O content of the structure here. In contrast, the range of angles explored by the O-C-O vector in the 1L structure of Ca-hectorite is larger than in the 1L structure of the same model exposed to dry $scCO_2$ at the same P and T.[42] This difference is most likely due to the combination of a slightly larger basal spacing (0.4Å) and a higher interlayer CO_2 mole fraction (1.0) with dry $scCO_2$ compared to our 1L simulations here (0.34) caused by the presence of interlayer H_2O. In the current study, the Ca^{2+} ions are coordinated by only H_2O molecules and basal oxygen atoms, which permits the intercalated CO_2 molecules to occupy the volume between hydrated metal cations. As also found in molecular simulations of Na-hectorite,[40] the intercalated CO_2 molecules in the Cs- and Ca-hectorite simulations do not undergo isotropic reorientation, as shown by the lack of peaks or shoulders near -1 and +1 for the O-C-O vectors. The average angles probed by the H_2O dipole vectors for the 1L and 2L structures of Ca-hectorite are similar to those in Na-hectorite, demonstrating two different H_2O orientations, consistent with the presence of two different types of interlayer H_2O (Figure S1 and related discussion in the Supporting Information).[40]

The radial distribution functions (RDFs) and running coordination numbers (RCNs; Figures 3a, 3c, 3e) clearly show that the intercalated CO_2 directly coordinates Cs^+ in the 1L

Cs-hectorite structure (Figure 3b) and that it does not coordinate Ca^{2+} in either the 1L or 2L structures, even for short times (Figures 3d and 3f). For the Cs-hectorite 1L structure, the mean Cs^+ - O_{CO2} and Cs^+ - O_b, interatomic distances are both ~3.2 Å. The Cs^+ - O_b RCN is 8.3, and the Cs^+ - O_{CO2} RCN is 4.5, resulting in a total ion coordination number of ~12.8. Each Cs^+ ion is in inner sphere (IS) coordination at the center of a ditrigonal cavity of one surface and above a Si tetrahedron on the other (Figure 3b), as well as being surrounded by 4-5 CO_2 molecules. The Cs^+ - O_{CO2} RCNs are essentially identical to those of Cs-hectorite exposed to dry $scCO_2$ under same thermodynamic conditions, as expected due to the low H_2O content here.[42] Importantly, the Cs^+- O_{CO2} RCN here is very similar to that of Cs^+- O_{H2O} in Cs-hectorite in equilibrium with pure H_2O.[49] This result is in good agreement with our recent experimental results, which suggest that replacement of H_2O by CO_2 in the 1L structure of Cs-hectorite under the conditions here requires only a small energy change.[17] The mean non-bonded O_{CO2} – O_b and O_{CO2} - O_{CO2} interatomic distances in Cs-hectorite are centered at 3.4 Å and 3.2 Å, respectively, and the O_{CO2}-O_b RCN is ~7.7 (Figure 4a). The average local structure of the CO_2 molecules is best characterized as having the O_{CO2} atoms located above a silica tetrahedron of one basal surface and above the center of a ditrigonal cavity of the other basal surface (Figure 3b). The O_{CO2}-O_{CO2} RCN is ~4.6, and their mutual arrangement is dominated by a slipped parallel arrangement (parallel CO_2 with slight offset) with only a small fraction of T-shaped arrangements (Figure 3b).[38] The rapid reorientation of CO_2 perpendicular to the O-C-O molecular axis is well illustrated by the dispersed contours for O_{CO2} in the 1L structure (Figure S2).

In both the 1L and 2L structures of Ca-hectorite, the mean Ca^{2+} - O_{H2O} distance is 2.5 Å, similar to the value in bulk aqueous solutions (Figure 3c and 3e),[75] and the absence of nearest neighbor cation-O_{CO2} coordination is the same as in Na-hectorite.[40] This later result is consistent with the expectation that cations with large hydration energies and smaller CO_2

solvation energies prefer to be coordinated by H_2O at all R.H.s.[58,75] In Ca-hectorite, the intercalated CO_2 molecules occur in small clusters between the hydrated Ca^{2+} ions (Figure 3d), as also observed in previous MD simulations of Na-montmorillonite.[38] The adsorption environment of the Ca^{2+} ions is very similar to our previous results of hydrated Ca-hectorite without CO_2.[51]

The local coordination environment of CO_2 in the 1L structure of Ca-hectorite is significantly different than in Cs-hectorite, with one O_{CO2} at the center of a ditrigonal cavity of one surface and the other directly above an O_b of the opposite basal surface (Figure 3d). The adsorption environment of CO_2 molecules reported here is in good agreement with earlier calculations for Na-hectorite under identical simulated conditions.[40] This structure is also in agreement with the O_{CO2}-O_b RCN of ~7.0 (Figure 4b). The aggregation of CO_2 is mostly in trimers (O_{CO2}-O_{CO2} RCN = 3.6) with a slipped parallel orientation. There is no evidence of T-shaped arrangements, as is also observed in the 1L structure of Cs-hectorite. The total non-bonded coordination of CO_2 in Ca-hectorite increases from 10.3 (7.1 O_b : 3.2 O_{H2O}) in the 1L structure to 12.3 (4.0 O_b : 8.3 O_{H2O}) in the 2L structure, but the H_2O coordination to O_b atoms in the 1L and 2L structures is nearly the same as in hydrated Ca-hectorite without CO_2.[51] This result demonstrates that the H_2O to O_b H-bonding is not significantly affected by the presence of CO_2. The mean O_b-O_{CO2} distances decrease from 3.6 Å to 3.3 Å as the basal spacing increases from the 1L to 2L structures, suggesting a more compact arrangement in the 2L structure. Despite having similar mean O_{CO2}-O_b and O_{CO2}-O_{H2O} interatomic distances, the RCN values in Ca-hectorite are significantly smaller than in the simulations of Ca-montmorillonite exposed to wet CO_2 fluid at 323 K and 90 bar due to the differences in layer charge and location, as discussed above.[34] The average adsorption environments of the intercalated species for cations, H_2O and CO_2 in the 1L and 2L structures of Cs- and Ca-hectorites are further

validated by the planar atomic density distributions discussed in the supporting information (Figures S2-S6).

Coordination times and dynamics of the interlayer species

The mean nearest neighbor coordination times among the different intercalated species (H_2O, CO_2, cations) and with surface O_b atoms show that the charge compensating cations play a crucial role in dictating the overall interlayer dynamics (Table 2). For the 1L structures, the intermittent and continuous coordination times for the Ca^{2+}-O_b pair are an order of magnitude longer than for the Cs^+-O_b pair, in good agreement with previous MD simulations of hydrated hectorites under ambient conditions.[51] In the 1L structures of both Cs- and Ca-hectorite, the cation-O_b coordination times are significantly longer than the O_{CO2}-O_b coordination times, reflecting the weaker interaction of the CO_2 with the clay surface compared to cations. In contrast, the O_{CO2} spend similar times near O_b and Cs^+ in the 1L structure, suggesting a constant exchange among these coordination environments. This exchange may be due to the reorientation of the CO_2 parallel to the surface, which is consistent with the delocalized PADD contours for CO_2 molecules (Figure S2). The O_{CO2}-O_{H2O} and O_{CO2}-O_b residence times are similar for both the 1L and 2L structure of Ca-hectorite, but these times are much shorter than those for Ca-O_{H2O} and Ca-O_b, indicating that the interactions of CO_2 with the surface and H_2O are weaker than those of Ca^{2+}. The longer coordination times of Ca^{2+} with H_2O than with O_b is consistent with its large hydration energy.[58] For Ca-hectorite, all the coordination times for the 2L structure are shorter than for the 1L structure, reflecting the higher probability for H_2O molecules to exchange between the 1st and 2nd coordination spheres of Ca^{2+} with CO_2 librating and hopping between surface sites. There are no residence time values for Ca-O_{CO2} for the 1L and 2L structures of Ca-hectorite and O_{H2O} coordination around Cs^+ and O_{CO2} in 1L structure of Cs-hectorite, because such coordination does not occur, even for short periods of time

(Figures 3c-3f). Similarly, because Ca^{2+} is present in outer sphere coordination in the 2L structure, there are no Ca-O_b values for it.

Conclusions

Our GCMD simulation studies indicate that the intercalation behavior of CO_2 and H_2O in the interlayers of hectorite when in contact with a binary H_2O-saturated $scCO_2$ fluid at 323 K and 90 bars strongly depends on the hydration and solvation properties of the exchangeable, charge compensating cations. The adsorption profiles provide direct evidence for CO_2 intercalation in Cs-hectorite even under anhydrous conditions, as observed in recent experimental studies.[17] In contrast, CO_2 intercalation in Ca-hectorite occurs only when there is at least a sub-monolayer of H_2O present in the interlayers, as is also the case for Na-smectites.[17,25] The maximum interlayer mole fraction for CO_2 occurs near the 1L structure for both Cs- (12.5 Å) and Ca-hectorites (12.8 Å) and decreases with increasing basal spacing. The negligible H_2O content (~1.5%) present at the maximum CO_2 content in Cs-hectorite clearly indicates that Cs^+ has similar affinities for both H_2O and CO_2, in good agreement with experiments.[17,58] The calculated immersion energies show that at the simulated conditions the 1L (12.5 Å) and 2L (16.2 Å) structures represent the stable equilibrium states for Cs- and Ca-hectorite, respectively.

The structural and dynamical behavior of the CO_2 molecules in the 1L and 2L structures are in full agreement with previous interpretations of ^{13}C NMR SSB patterns.[17] The simulations show that CO_2 molecules in the 1L structures are located at the interlayer midplane, have a mean O-C-O axis orientation parallel to the basal surface (though they wobble around this mean value), and undergo librational motion about an axis perpendicular to their O-C-O axis. The observed ^{13}C MAS NMR CSA patterns demonstrate rapid reorientation about an axis perpendicular to their O-C-O axis and because they probe the time-averaged structure are consistent with wobbling around this axis.[17] In contrast, simulations show that the intercalated

CO_2 molecules in the 2L structure of Ca-hectorite are adsorbed closer to one of the basal surfaces and experience less restricted dynamics than in the 1L structure. The computations show that direct, nearest neighbor coordination of CO_2 with Cs^+ in the 1L structure, but no nearest neighbor CO_2-Ca^{2+} coordination in either the 1L or 2L structures of Ca-hectorite. Again, these results are in full agreement with *in situ* experimental NMR observations.[17] In the 1L structure of Cs-hectorite Cs^+ ions are adsorbed in a 9-fold IS coordination with respect to the basal surfaces and are also coordinated to 4-5 CO_2. In contrast, in the 1L structure of Ca-hectorite CO_2 molecules occur exclusively in small clusters between hydrated Ca^{2+} ions, where they assume a predominantly slipped parallel orientation with respect to each other. In the 1L structure of Cs-hectorite, the CO_2 molecules have one O_{CO2} above a Si tetrahedron of one surface and the other above the center of a ditrigonal cavity of the opposite surface. This arrangement is slightly altered in both the 1L and 2L structures of Ca-hectorite, in which one O_{CO2} is above the center of a ditrigonal cavity but the other is above an O_b on the opposite surface and not on top of a Si tetrahedron.

Overall, the computed intercalation structure, dynamics and compositions are in good agreement with the recent *in situ* XRD, IR and NMR experimental data of Bowers et al.[17], highlighting the complementarity of spectroscopy and molecular modeling. The agreement between the experimental interpretations and those observed in the GCMD simulations suggests that GCMD methods can be broadly applicable in future studies of binary and more complex fluids in complex nanoconfined environments.

Acknowledgements

All the calculations in this work were performed using computational resources at the National Energy Research Scientific Computing Center, which is supported by the Office of Science of the U.S. Department of Energy under ECARP No. m1649. The authors acknowledge iCER computational facility at Michigan State University for additional computational

resources. The work in this manuscript was supported by the United States Department of Energy, Office of Science, Office of Basic Energy Science, Chemical science, Biosciences, and Geosciences division through the sister grants DE-FG02-10ER16128 (Bowers, P.I.) and DE-FG02-08ER15929 (Kirkpatrick, P.I.). A.G.K. acknowledges financial support of the industrial chair "Storage and Disposal of Radioactive Waste" at the IMT-Atlantique, funded by ANDRA, Areva, and EDF, and of the European Union's Horizon 2020 research and innovation program under grant agreements No. 640979 and 764810.

Notes

The authors declare no competing financial interest.

Supporting Information

A brief discussion of residence time definitions, orientations of H2O dipole with respect to surface normal of Ca-hectorites for 1L and 2L structures. Details of the planar atomic density distributions of interlayer species for the 1L and 2L structures of Cs- and Ca-hectorites.

References

1. Gauss, I. Role and Impact of CO_2-Rock Interactions during CO_2 Storage in Sedimentary Rocks. *Int. J. Green. Gas Cont.* **2010,** 4, 73-89.
2. Lackner, K. S. A Guide to CO_2 Sequestration. *Science* **2003,** *300*, 1677-1678.
3. Benson, S. M.; Cole, D. R. CO_2 Sequestration in Deep Sedimentary Formations. *Elements* **2008,** 4, 325-331.
4. Rutqvist, J. The Geomechanics of CO_2 Storage in Deep Sedimentary Formations. *Geotech. Geol. Eng.* **2012,** 30, 525-551.
5. Bickle, M. J. Geological Carbon Storage. *Nature Geosci.* **2009,** 2, 815-818.
6. Plasynski, S. I.; Litynski, J.T.; Mcllvried, H. G.; Vikara, D. M.; Srivastava, R. D. The Critical Role of Monitoring, Verification, and Accounting for Geological Carbon Dioxide Storage Projects. *Environ. Geosci.* **2011,** 18, 19-34.
7. Bachu, S.; Bonijoly, D.; Bradshaw, J.; Burruss, R.; Holloway, S.; Christensen, N. P.; Mathiassen, O. M. CO_2 Storage Capacity Estimation: Methodology and Gaps. *Int. J. Green. Gas Cont.* **2007,** 1, 430-443.
8. Bourg, I. C.; Beckingham, L. E.; DePaolo, D. J. Then Nanoscale Basis of CO_2 Trapping for Geologic Storage. *Environ. Sci. Technol.* **2015,** 49, 10265-10284.
9. Edlmann, K.; Haszeldine, S.; McDermott, C. I. Experimental Investigation into Sealing Capability of Naturally Fractured Shale Caprocks to Supercritical Carbon Dioxide Flow. *Environ. Earth Sci.* **2013,** 70, 3393-3409.
10. Cole, D. R.; Chialvo, A. A.; Rother, G.; Vlcek, L.; Cummings, P. T. Supercritical Fluid Behavior at Nanoscale Interfaces: Implications for CO_2 Sequestration in Geological Formations. *Philoso. Mag.* **2010,** 90, 2339-2363.
11. Berrezueta, E.; Menendez, G-, L.; Breitner, D.; Luquot, L. Pore System Changes During Experimental CO_2 Injection into Detritic Rocks. Studies of Potential Storage Rocks from Some Sedimentary Basins of Spain. *Int. J. Green. Gas Cont.* **2013,** 4, 73-89
12. Ross, D. J. K.; Bustin, R. M. The Importance of Shale Composition and Pore Structure upon Gas Storage Potential of Shale Gas Reservoirs. *Mari. Petro. Geo.* **2009,** 26, 916-927.
13. Heller, R.; Zoback, M. Adsorption of Methane and Carbon Dioxide on Gas Shale and Pure Mineral Samples. *J. Unconv. Oil Gas Res.* **2014,** 8, 14-24.
14. Middleton, R. S.; Carey J. W.; Currier, R. P.; Hyman, J. D.; Kang, Q.; Karra, S.; Martinez, J. J-.; Porter, M. L.; Viswanathan, H. S. Shale Gas and Non-Aqueous Fracturing Fluid: Opportunities and Challenges for Supercritical CO_2. *Appl. Ener.* **2015,** 147, 500-509.
15. Busch, A.; Bertier, P.; Gensterblum, Y.; Rother, G.; Spiers, C. J.; Zhang, M.; Wentinck, H. M. On Sorption and Swelling of CO_2 in Clays. *Geomech. Geophys. Geo-energ. Geo-resour.* **2016,** *2*, 111-130.
16. Hamm, L. M.; Bourg, I. C.; Wallace, A. F.; Rotenberg, B. Molecular Simulation of CO_2- and CO_3-Brine-Mineral Systems. *Reviews in Mineralogy and Geochemistry* **2013,** *77*, 189-228.
17. Bowers, G. M.; Schaef, H. T.; Loring, J. S.; Hoyt, D. W.; Burton, S. D.; Walter, E. D.; Kirkpatrick, R. J. Role of Cations in CO_2 Adsorption, Dynamics and Hydration in Smectite Clays under In Situ Supercritical CO_2 Conditions. *J. Phys. Chem. C* **2017,** *121*, 577-592.

18. Giesting, P.; Guggenheim, S.; van Groos, A. F. K.; Busch, A. Interaction of Carbon Dioxide with Na-Exchanged Montmorillonite at Pressures to 640 bar: Implications for CO_2 Sequestration. *Int. J. Green. Gas Cont.* **2012,** 8, 73-81.

19. Giesting, P.; Guggenheim, S.; van Groos, A. F. K.; Busch, A. X-ray Diffraction Study of K- and Ca-Exchanged Montmorillonites in CO_2 Atmospheres. *Environ. Sci. Technol.* **2012,** 46, 5623-5630.

20. Bowers, G. M.; Hoyt, D. W.; Burton, S. D.; Ferguson, B. O.; Varga, R.; Kirkpatrick, R. J. In Situ ^{13}C and ^{23}Na Magic Angle Spinning NMR Investigation of Supercritical CO_2 Incorporation in Smectite-Natural Organic Matter Composites. *J. Phys. Chem. C* **2014,** *118*, 3564-3573.

21. Wang, Z.; Felmy, A. R.; Thompson, C. J.; Loring, J. S.; Joly, A. G.; Rosso, K. M.; Schaef, H. T.; Dixon, D. A. Near-Infrared Spectroscopic Investigation of Water in Supercritical CO_2 and the effect of $CaCl_2$. *Fluid Phase Equil.* **2013,** *338*, 155-163.

22. Lee, M.-S.; McGrail, B. P.; Glezakou, V.-A. Microstructural Response of Variably Hydrated Ca-rich Montmorillonite to Supercritical CO_2. *Environ. Sci. Technol.* **2014,** 48, 8612-8619.

23. Ilton, E. S.; Schaef, H. T.; Qafoku, O.; Rosso, K. M.; Felmy, A. R. In Situ X-ray Diffraction Study of Na^+ Saturated Montmorillonite Exposed to Variably Wet Supercritical CO_2. *Environ. Sci. Technol.* **2012,** 46, 4241-4248.

24. Guggenheim, S.; van Groos, A. F. K. An Integrated Experimental System for Solid-Gas-Liquid Environmental Cells. *Clays Clay Miner.* **2014,** 62, 470-476.

25. Rother, G.; Ilton, E. S.; Wallacher, D.; Hauss, T.; Schaef, H. T.; Qafoku, O.; Rosso, K. M.; Felmy, A. R.; Krukowski, E. G.; Stack, A. G.; et al. CO_2 Sorption to Subsingle Hydration Layer Montmorillonite Clay Studies by Excess Sorption and Neutron Diffraction Measurements. *Environ. Sci. Technol.* **2013,** 47, 205-211.

26. Schaef, H. T.; Ilton, E. S.; Qafoku, O.; Martin, P. F.; Felmy, A. R.; Rosso, K. M. In Situ X-RD study of Ca^{2+} Saturated Montmorillonite (STx-1) Exposed to Anhydrous and Wet Supercritical Carbon Dioxide. *Int. J. Green. Gas Cont.* **2012,** 6, 220-229.

27. Romanov, V. N. Evidence of Irreversible CO_2 Intercalation in Montmorillonite. *Int. J. Green. Gas Cont.* **2013,** 14, 220-226.

28. Schaef, H. T.; Loring, J. S.; Glezakou, V. A.; Miller, Q. R. S.; Chen, J.; Owen, A. T.; Lee, M.-S.; Ilton, E. S.; Felmy, A. R.; McGrail, B. P. et al. Competitive Sorption of CO_2 and H_2O in 2:1 Layer Phyllosilicates. *Geochim. Cosmochim. Acta* **2015,** 161, 248-257.

29. Loring, J. S.; Schaef, H. T.; Turcu, R. V. F.; Thompson, C. J.; Miller, Q. R.; Martin, P. F.; Hu, J.; Hoyt, D. W.; Qafoku, O.; Ilton, E. S.; et al. In Situ Molecular Spectroscopic Evidence for CO_2 Intercalation into Montmorillonite in Supercritical Carbon Dioxide. *Langmuir* **2012,** *28*, 7125-7128.

30. Loring, J.S.; Ilton, E.S.; Chen, J.; Thompson, C.J.; Martin, P.F.; Benezeth, P.; Rosso, K.M.; Felmy, A.R.; Schaef, H.T. In Situ Study of CO_2 and H_2O Partitioning Between Na-Montmorillonite and Variably Wet Supercritical Carbon Dioxide. *Langmuir* **2014,** *30*, 6120-6128.

31. Loring, J. S.; Schaef, H. T.; Thompson, C. J.; Turcu, R. V. F.; Miller, Q. R.; Chen, J.; Hu, J.; Hoyt, D. W.; Martin, P. F.; Ilton, E. S.; et al. Clay Hydration/Dehydration in Dry to

Water-Saturated Supercritical CO_2: Implications for Caprock Integrity. *Energy Procedia* **2013,** *37*, 5443-5448.

32. Krukowski, E.G.; Goodman, A.; Rother, G.; Ilton, E.S.; Guthrie, G.; Bodnar, R.J. FT-IR Study of CO_2 Interaction with Na^+ Exchanged Montmorillonite. *Appl. Clay Sci.* **2015,** *114*, 61-68.
33. Botan, A.; Rotenberg, R.; Marry, V.; Turq, P.; Noetinger, B. Carbon Dioxide in Montmorillonite Clay Hydrates: Thermodynamics, Structure and Transport from Molecular Simulation. *J. Phys. Chem. C* **2010**, *114*, 14962-14969.
34. Kadoura, A.; Nair, A. K. N.; Sun, S. Molecular Simulation Study of Montmorillonite in Contact with Variably Wet Supercritical Carbon Dioxide. *J. Phys. Chem. C* **2017**, *121*, 6199-6208.
35. Myshakin, E. M.; Saidi, W. A.; Romanov, V. N.; Cygan, R. T.; Jordan, K. D. Molecular Dynamics Simulations of Carbon Dioxide Intercalation in Hydrated Na-Montmorillonite. *J. Phys. Chem. C* **2013**, *117*, 11028-11039.
36. Makaremi, M.; Jordan, K. D.; Guthrie, G. D.; Myshakin, E. M. Multiphase Monte Carlo and Molecular Dynamics Simulations of Water and CO_2 Intercalation in Montmorillonite and Beidellite. *J. Phys. Chem. C* **2015**, *119*, 15112-15124.
37. Rao, A.; Leng, Y. Effect of Layer Charge on CO_2 and H_2O Intercalations in Swelling Clays. *Langmuir* **2016**, *32*, 11366-11374.
38. Sena, M. M.; Morrow, C. P.; Kirkpatrick, R. J.; Krishnan, M. Structure, Energetics, and Dynamics of Supercritical Carbon Dioxide at Smectite Mineral-Water Interfaces: Molecular Dynamics Modeling and Adaptive Force Investigation of CO_2/H_2O Mixtures Confined in Na-Montmorillonite. *Chem. Mater.* **2015**, *27*, 6946-6959.
39. Yazaydin, A. O.; Bowers, G. M.; Kirkpatrick, R. J. Molecular Dynamics Modeling of Carbon Dioxide, Water and Natural Organic Matter in Na-Hectorite. *Phys. Chem. Chem. Phys.* **2015**, *17*, 23356-23367.
40. Loganathan, N.; Yazaydin, A. O.; Bowers, G. M.; Kalinichev, A. G.; Kirkpatrick, R. J. Molecular Dynamics Study of CO_2 and H_2O Intercalation in Smectite Clays: Effect of Temperature and Pressure on Interlayer Structure and Dynamics in Hectorite *J. Phys. Chem. C* **2017**, *121*, 24527-24540.
41. Schaef, H. T.; Loganathan, N.; Bowers, G. M.; Kirkpatrick, R.; Yazaydin, A. O.; Burton, S. D.; Hoyt, D. W.; Ilton, E. S.; Thanthiriwatte, K. S.; Dixon, D. A. et al. Tipping Point for Expansion of Layered Aluminosilicates in Weakly Polar Solvents: Supercritical CO_2. *ACS Appl. Mater. Interf.* **2017**, *9*, 36783-36791.
42. Loganathan, N.; Bowers, G. M.; Yazaydin, A. O.; Schaef, H. T.; Loring, J.; Kalinichev, A. G.; Kirkpatrick, R. J. Clay Swelling in Dry Supercritical Carbon Dioxide: Effects of Interlayer Cations on the Structure, Dynamics and Energetics of CO_2 Intercalation Probed by XRD, NMR and GCMD Simulations. *J. Phys. Chem. C* **2018**, *122*, 4391-4402.
43. Bowers, G. M.; Singer, J. W.; Bish, D. L.; Kirkpatrick, R. J. Alkali Metal and H_2O Dynamics at the Clay/Water Interface. *J. Phys. Chem. C* **2011**, *115*, 23395-23407.
44. Marry, V.; Dubois, E.; Malikova, N.; Durand-Vidal, S.; Longeville, S.; Breu, J. Water Dynamics in Hectorite Clays: Influence of Temperature Studied by Coupling Neutron Spin Echo and Molecular Dynamics. *Environ. Sci. Technol.* **2011**, *45*, 2850-2855.

45. Bowers, G. M.; Singer, J. W.; Bish, D. L.; Kirkpatrick, R. J. Structure and Dynamical Relationships of Ca^{2+} and H_2O in Smectite/^2H_2O Sytems. *Amer. Mineral*. 2014, *99*, 318-331.

46. Weiss, C. A.; Kirkpatrick, R. J.; Altaner, S. P. Variations in Interlayer Cation Sites of Clay Minerals as Studied by ^{133}Cs MAS Nuclear Magnetic Resonance Spectroscopy. *Amer. Mineral*. **1990**, *75*, 970-982.

47. Weiss, C. A.; Kirkpatrick, R. J.; Altaner, S. P. The Structural Environments of Cations Adsorbed onto Clays – ^{133}Cs Variable-Temperature MAS NMR Spectroscopic Study of Hectorite. *Geochim. Cosmochim. Acta* **1990**, *54*, 1655-1669.

48. Reddy, U. V.; Bowers, G. M.; Loganathan, N.; Bowden, M.; Yazaydin, A. O.; Kirkpatrick, R. J. Water Structure and Dynamics in Smectites: ^2H NMR Spectroscopy of Mg, Ca, Sr, Cs and Pb-Hectorite. *J. Phys. Chem. C* **2016,** *120*, 8863-8876.

49. Loganathan, N.; Yazaydin, A. O.; Bowers, G. M.; Kalinichev, A. G.; Kirkpatrick, R. J. Structure, Energetics and Dynamics of Cs^+ and H_2O in Hectorite: Molecular Dynamics Simulations with Unconstrained Substrate Surface. *J. Phys. Chem. C* **2016**, 1*20*, 10298-10310.

50. Porion, P.; Faugere, A. M.; Delville, A. Multiscale Water Dynamics within Dense Clay Sediments Probed by ^2H Multiquantum NMR Relaxometry and Two-Time Stimulated Echo NMR Spectroscopy. *J. Phys. Chem. C* **2013**, *117*, 26119-26134.

51. Loganathan, N.; Yazaydin, A. O.; Bowers, G. M.; Kalinichev, A. G.; Kirkpatrick, R. J. Cation and Water Structure, Dynamics and Energetics in Smectite Clays: A Molecular Dynamics Study of Ca-Hectorite *J. Phys. Chem. C* **2016**, *120*, 12429-12439.

52. Morrow, C. P.; Yazaydin, A. O.; Krishnan, M.; Bowers, G. M.; Kalinichev, A. G.; Kirkpatrick. R. J. Structure, Energetics and Dynamics of Smectite Clay Interlayer Hydration: Molecular Dynamics and Metadynamics Investigation of Na-Hectorite. *J. Phys. Chem. C* **2013**, *117*, 5172-5187.

53. Greathouse, J. A.; Hart, D. B.; Bowers, G. M.; Kirkpatrick, R. J.; Cygan, R. T. Molecular Simulation of Structure and Diffusion at Smectite-Water Interfaces: Using Expanded Clay Interlayers as Model Nanopores. *J. Phys. Chem. C* **2015**, *119*, 17126-17136.

54. Ngouana-Wakou. B.F.; Kalinichev, A.G. Structural Arrangements of Isomorphic Substitutions in Smectites: Molecular Simulation of the Swelling Properties, Interlayer Structure and Dynamics of Hydrated Cs-Montmorillonite Revisited with New Clay Models. *J. Phys. Chem. C* **2014**, *118*, 12758-12773.

55. Loganathan, N.; Kalinichev, A. G. On the Hydrogen Bonding Structure at the Aqueous Interface of Ammonium-Substituted-Mica: A Molecular Dynamics Simulation. *Z. Naturforsch., A: Phys. Sci.* **2013,** *68a*, 91-100.

56. Sato, T.; Watanabe, T.; Otuka, R. Effects of Layer Charge, Charge Location, and Energy Change on Expansion Properties of Dioctahedral Smectites. *Clays Clay Miner.* **1992**, *29*, 873-882.

57. Loganathan, N.; Kalinichev, A. G. Quantifying the Mechanisms of Site-Specific Ion Exchange at an Inhomogeneously Charged Surface. Case of Cs^+/K^+ on Hydrated Muscovite Mica *J. Phys. Chem. C* **2017**, *121*, 7829-7836.

58. Criscenti, L. J.; Cygan, R. T., Molecular Simulations of Carbon Dioxide and Water: Cation Solvation. *Environ. Sci. Technol.* **2013**, *47*, 87-94.

59. Breu, J.; Seidl, W.; Stoll, A., Disorder in Smectites in Dependence of the Interlayer Cation. Z. *Anorg. Allg. Chem*. **2003**, *629*, 503-515.

60. Tenorio, R. P.; Alme, L. R.; Engelsberg, M.; Fossum, J. O.; Hallwass, F. Geometry and Dynamics of Intercalated Water in Na-Fluorohectorite Clay Hydrates. *J. Phys. Chem. C* **2008**, *112*, 575-580.

61. Lowenstein, W. The Distribution of Aluminium in the Tetrahedra of Silicates and Aluminates. *Am. Mineral*. **1954**, *39*, 92-96.

62. Boinepalli, S.; Attard, P. Grand Canonical Molecular Dynamics. *J. Chem. Phys*. **2003**, *119*, 12769-12775.

63. Dubbeldam, D.; Calero, S.; Ellis, D. E.; Snurr, R. Q. RASPA: Molecular Simulation Software for Adsorption and Diffusion in Flexible Nanoporous Materials. *Mol. Simul.* **2016**, *42*, 81-101.

64. Cygan, R. T.; Liang, J.-J.; Kalinichev, A. G. Molecular Models of Hydroxide, Oxyhydroxide and Clay Phases and the Development of a General Force Field. *J. Phys. Chem. B* **2004,** *108*, 1255-1266.

65. Berendsen, H. J. C.; Postma, J. P. M.; Gunsteren, W. F.; van Hermans, J. Interaction Models for Water in Relation to Protein Hydration. In *Intermolecular Forces*; The Jerusalem Symposia on Quantum Chemistry and Biochemistry; Pullman, B., Ed.; Springer: Netherlands, 1981; pp 331−342.

66. Cygan, R. T.; Romanov, V. N.; Myshakin, E. M. Molecular Simulation of Carbon Dioxide Capture by Montmorillonite Using an Accurate and Flexible Force Field. *J. Phys. Chem. C* **2012,** *116*, 13079-13091.

67. Allen, M. P.; Tildesley, D. J. Computer Simulations of Liquids; 2nd edition. Oxford University Press: Oxford, U.K., 2017.

68. Spycher, N.; Pruess, K.; Ennis-King J. CO_2-H_2O Mixtures in the Geological Sequestration fom 12 to 100º and up to 600 bar. *Geochim. Cosmochim. Acta* **2003,** *67*, 3015-3031.

69. Peng, D. Y.; Robinson, D. B. A New Two-Constant Equation of State. *Ind. Eng. Chem. Fundam.* **1976,** *15*, 59-64.

70. Smith, D. E. Molecular Computer Simulations of the Swelling Properties and Interlayer Structure of Cesium Montmorillonite. *Langmuir* **1998**, *14*, 5959-5967.

71. Young, D. A.; Smith, D. E. Simulations of Clay Mineral Swelling and Hydration: Dependence upon Interlayer Ion Size and Charge. *J. Phys. Chem. B* **2000**, *104*, 9163-9170.

72. Shroll, R.; Smith, D. E. Molecular Dynamics Simulations in the Grand Canonical Ensemble: Application to Clay Mineral Swelling. *J. Chem. Phys.* **1999**, *111*, 9025-9033.

73. Whitley, H. D.; Smith, D. E. Free Energy, Energy and Entropy of Swelling in Cs-, Na-, and Sr-Montmorillonite Clays. *J. Chem. Phys.* **2004**, *120*, 5387-5395.

74. Dazas, B.; Lanson, B.; Breu, J.; Robert, J.-L.; Pelletier, M.; Ferrage, E. Smectite Fluorination and its Impact on Interlayer Water Content and Structure: A Way to Fine Tune the Hydrophilicity of Clay Surfaces. *Micro. Meso. Mat.* **2013,** *181*, 233-247.

75. Ohtaki, H.; Radnai, T. Structure and Dynamics of Hydrated Ions. *Chem. Rev.* **1993,** *93*, 1157-1204.

Table 1. CO_2 mole fraction at equilibrium interlayer distances for Cs- and Ca-hectorites at 323 *K* and 90 bar in comparison to experimental results.

	Interlayer distance	**Interlayer mole fraction of CO_2**	
		(Simulations)	**(Experiments)[17]**
Cs – hectorite	Monolayer (12.5 Å)	0.98	0.34 - 0.82 (12.2 Å)
Ca – hectorite	Monolayer (12.7 Å)	0.34	0.13 - 0.54 (12.0 Å)
	Bilayer (16.2 Å)	0.02	0.02 - 0.42 (15.8 Å)
Na – hectorite	Monolayer (12.5 Å)[40]	0.18	0.05 - 0.14
	Bilayer (15.5 Å)[40]	0.03	

Table 2. Calculated intermittent and continuous residence times (*ns*) for the listed atomic pairs in the interlayers of Cs- and Ca-hectorite at 323 K and 90 bar.

basal spacing (Å)	Ion-O_{H2O}	Ion-O_b	Ion-O_{CO2}	O_{H2O}-O_b	O_b-O_{CO2}	O_{H2O}-CO_2
			τ_{int} (res): τ_{cont} (res)			
Ca-hectorite						
1L (12.8Å)	21 : 3	12 : 1	- : -	2 : 0.4	0.5 : 0.05	0.5 : 0.1
2L (16.2Å)	1.9 : 0.5	- : -	- : -	0.4 : 0.1	0.1 : 0.03	0.1 : 0.02
Cs-hectorite						
1L (12.5Å)	- : -	0.9 : 0.05	0.4 : 0.02	- : -	0.5 : 0.03	- : -

FIGURES

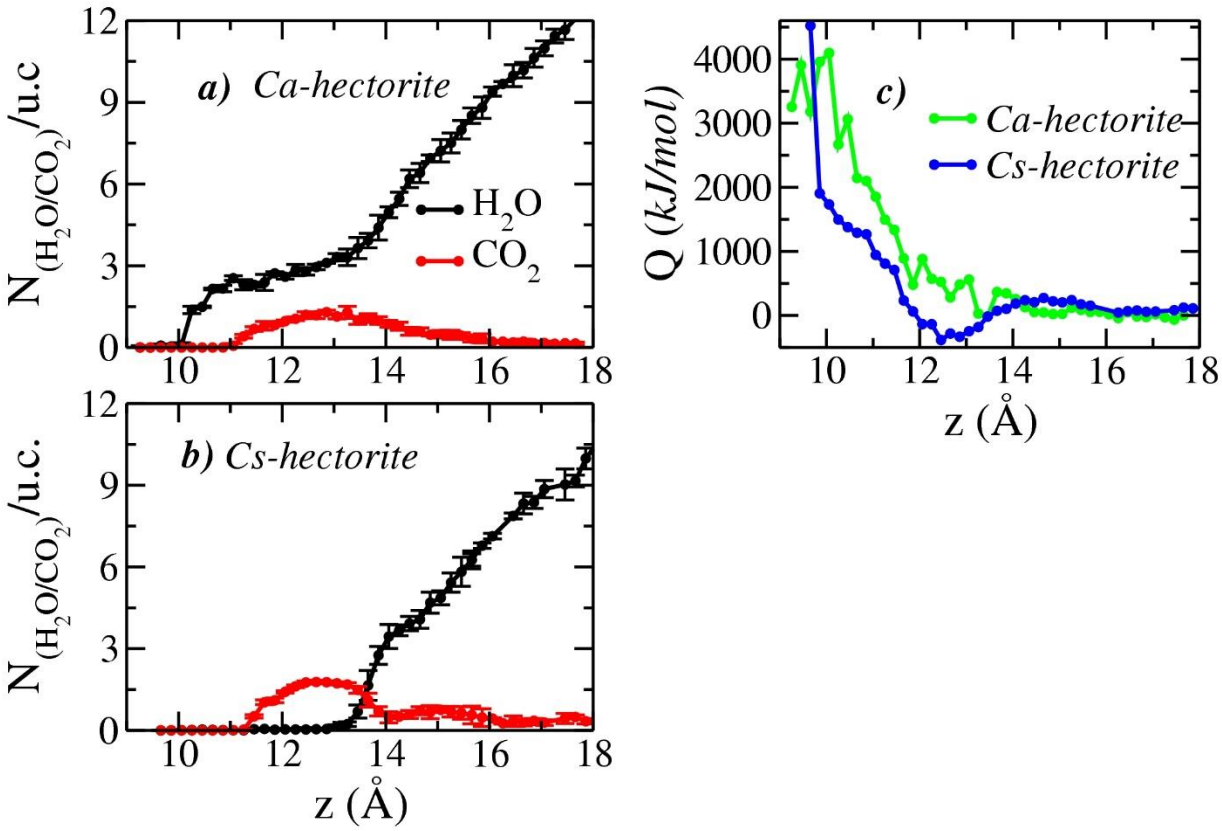

Figure 1. a) and b): Average number of intercalated CO_2 and H_2O molecules per unit cell in Ca- and Cs-hectorite as functions of interlayer basal spacing at 323 K and 90 bar. c): The computed immersion energies for the same systems.

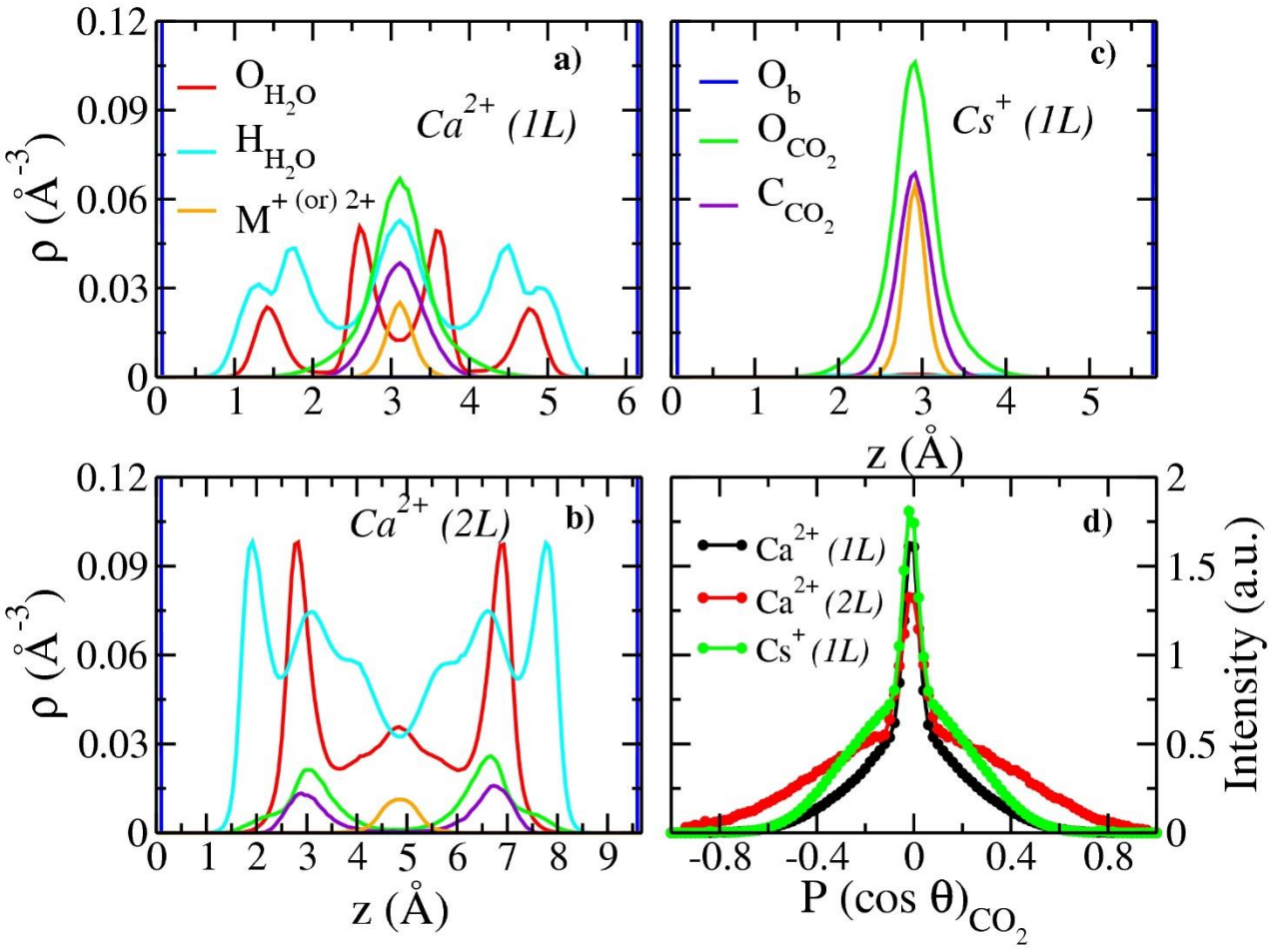

Figure 2. a), b), c): Computed atomic density profiles (ADPs) of O_b (dark blue vertical lines), the exchangeable cation (orange), O_{H2O} (red), H_{H2O} (cyan), O_{CO2} (green) and C_{CO2} (violet) in Cs- and Ca-hectorite as functions of distance from the basal clay surface at 323 K and 90 bar. a) and b) 1L and 2L structures of Ca-hectorite. The ADPs of O_{CO2} and C_{CO2} in 2b are enhanced 5 times than their original values to improve visibility. c) 1L structure of Cs-hectorite. d) Computed orientation distributions of intercalated CO_2 molecules in the interlayers of Ca- and Cs-hectorite at 323 K and 90 bar. P (cos θ)$_{CO2}$ is the cosine of the angle between the O-O vector of the CO_2 molecules and the normal to the hectorite basal surface. The intensity of the distribution for the 2L Ca-hectorite is enhanced 10X for better illustrations.

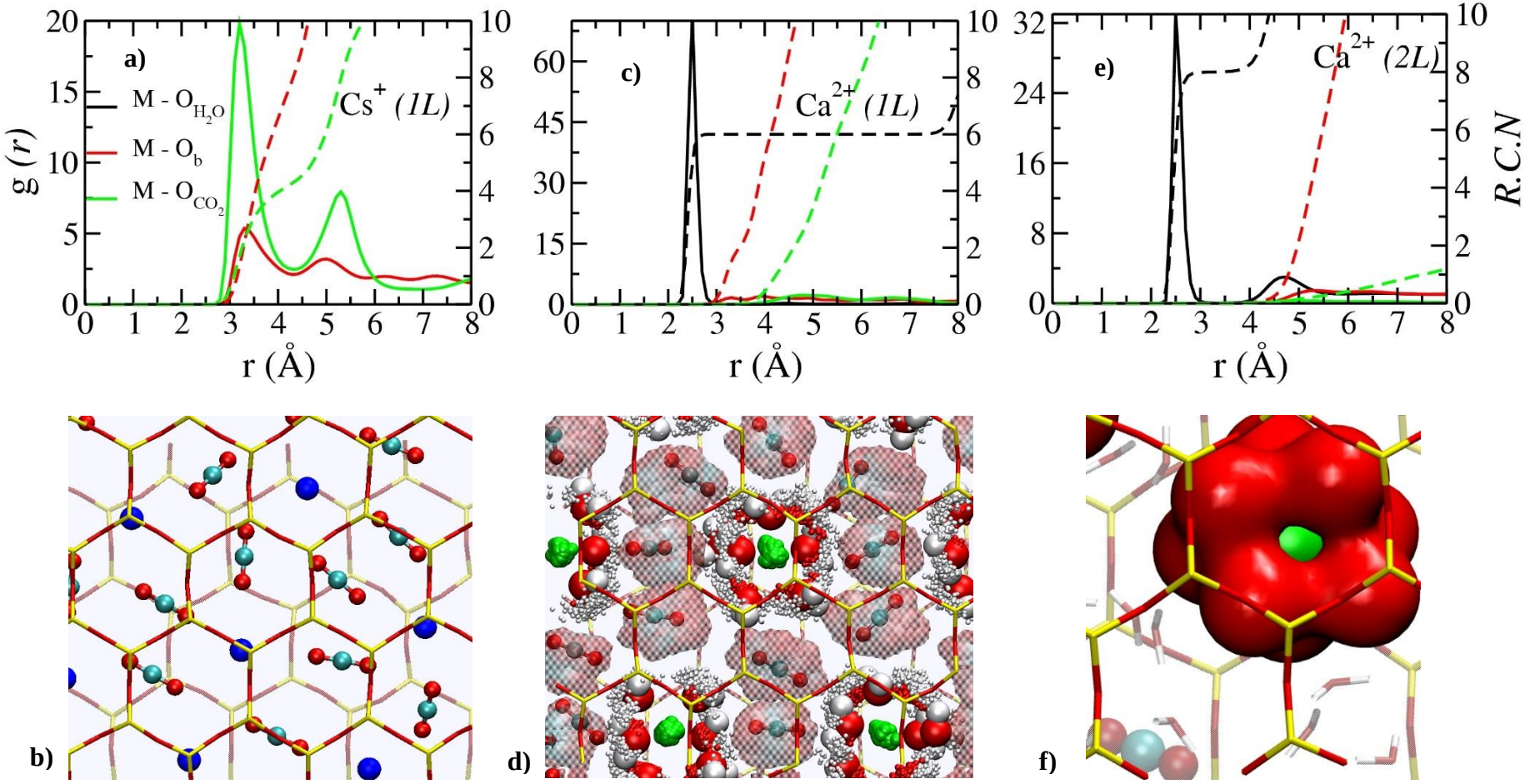

Figure 3. a), c), e): Radial distribution functions (RDFs, solid lines) and corresponding running coordination numbers (RCNs, dashed lines) for the indicated atomic pairs involving Cs^+ and Ca^{2+} ions in the interlayers of hectorite at 323 K and 90 bar. a) 1L of Cs-hectorite. b) 1L of Ca-hectorite. c) 2L of Ca-hectorite. M – Cation. b) pictorial representation of intercalated CO_2 and Cs^+ in 1L structure of Cs-hectorite; d) pictorial

representation of average positions for CO_2, H_2O and Ca^{2+} in 1L Ca-hectorite; f) pictorial representation of nearest neighbour H_2O around Ca^{2+} ions in 2L Ca-hectorite. Color codes: blue – Cs^+; green – Ca^{2+}; red – O_{H2O}/O_{CO2}; cyan – C_{CO2}; white – H_{H2O}; Bright and shaded red and yellow sticks corresponds to surface oxygen (O_b) and silicon atoms.

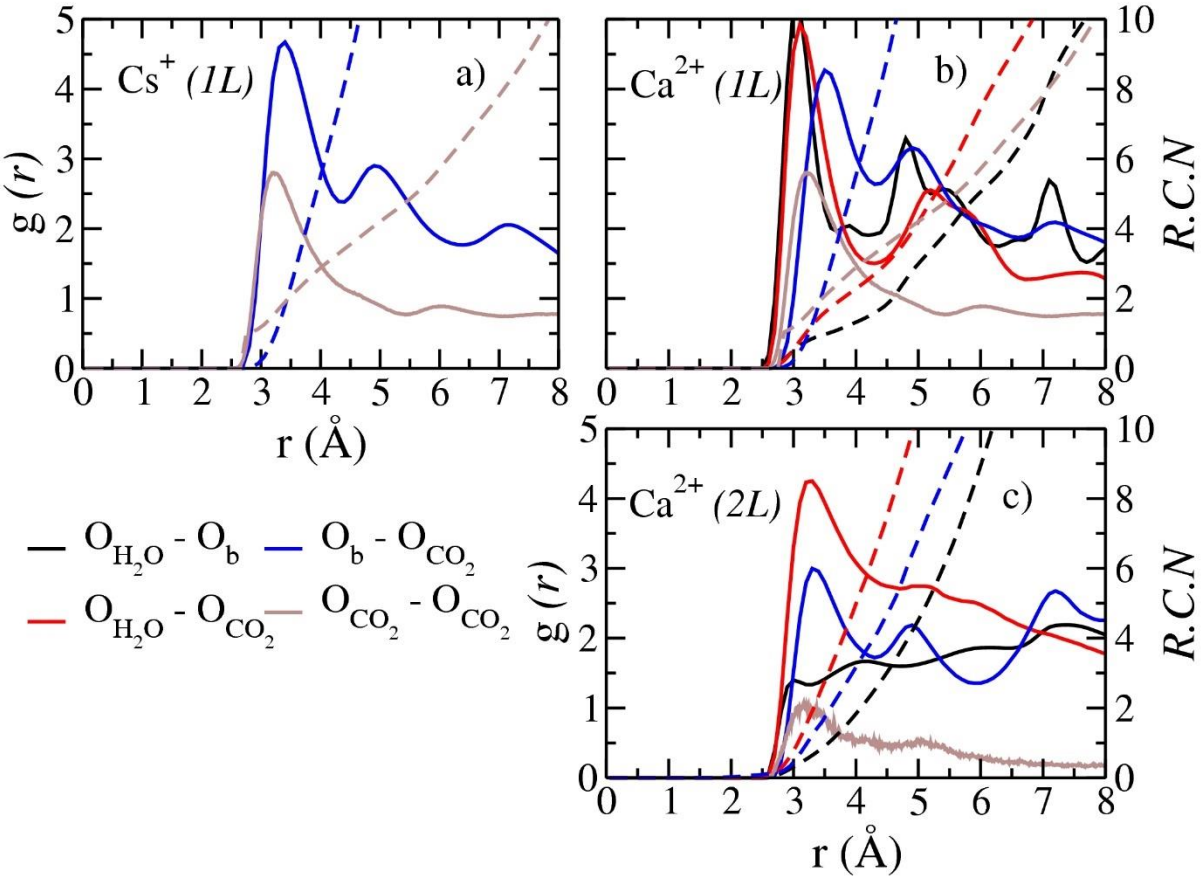

Figure 4. Radial distribution functions (RDFs, solid lines) and corresponding running coordination numbers (RCNs, dashed lines) for non-bonded O atomic pairs in Cs- and Ca-hectorites at 323 K and 90. a) 1L of Cs-hectorite. b) 1L of Ca-hectorite. c) 2L of Ca-hectorite.

TOC Graphic